International Journal on Advanced Science Engineering Information Technology

Vol.13 (2023) No. 5
ISSN: 2088-5334

Assessment of Extreme Precipitation for Developing Agricultural Adaptation Strategy in the Selo Watershed Area

Sugeng Nugroho [a], Rudi Febriamansyah [a,*], N. Nurhamidah [b], Dodo Gunawan [c]

[a] *Faculty of Agriculture Andalas University, Padang, West Sumatra, Indonesia*
[b] *Department of Civil Engineering, Faculty of Engineering Andalas University, Padang, West Sumatra, Indonesia*
[c] *Meteorological, Climatological, and Geophysical Agency, Climate Change Information Center, Jakarta, Indonesia*
*Corresponding author: *r_febriamansyah@agr.unand.ac.id*

Abstract*— The ongoing climate change resulting from the effects of global warming is manifested through increased variability and a rise in extreme precipitation events. Given this situation, it becomes imperative for farmers to adapt to these changes to ensure the long-term sustainability of their businesses. Therefore, this research aimed to assess extreme precipitation for planning adaptation strategies for agricultural water resources in the Selo watershed, Tanah Datar Regency, West Sumatra Province, Indonesia. Climate Hazards Group Infrared Precipitation and Stations (CHIRPS) data were used to accomplish this, spanning 1981 to 2020. A set of indices recommended by ETCCDI, including PRCPTOT, CDD, CWD, R95p, R99p, SDII, R10mm, R20mm, R30mm, and R40mm were employed to assess extreme precipitation. Climate Data Operator (CDO) and GrADS were conducted for downscale and plotting data. Furthermore, the Mann-Kendall test was conducted to determine the significance of change trends in the indices. R-Climdex was used to determine the extreme event based on the data used. The results showed that all indices indicated wet conditions during the period 1981-2020. The topographic characteristics of the watershed served as a basis for selecting suitable adaptation strategies within the agricultural water resources sector. One potential approach involves integrating conservation-based adaptation practices with comprehensive watershed management techniques. Factors such as the area's sensitivity to changes in the total intensity or frequency of precipitation, combined with the local environmental conditions, can be considered in determining the optimal adaptation approach.

***Keywords*— CHIRPS; ETCCDI; extreme precipitation indices; Mann-Kendall test; adaptation water resources.**

Manuscript received 24 May 2023; revised 30 Aug. 2023; accepted 28 Sep. 2023. Date of publication 31 Oct. 2023.

I. INTRODUCTION

The increase in greenhouse gas (GHG) concentration within the atmosphere is attributed to natural and human-induced factors and is the primary cause of climate change. However, due to anthropogenic activities, climate change has accelerated considerably, as stated by IPCC in 2007. The growing trend of GHG concentration is a significant indication of this phenomenon. One key species is carbon dioxide (CO2), monitored by the Global Atmosphere Watch (GAW) Station in Bukit Kototabang. The data obtained from the GAW Station shows an alarming 11% increase in CO2 concentration from 372 ppm in 2004 to 414 ppm in 2022 (https://bmkg.go.id/kualitas-udara/?p=gas-rumah-kaca, accessed on April 21, 2023). This is a concerning trend that must be addressed to mitigate the impact of climate change on a global scale.

Climate change manifested through changes in precipitation patterns, heightened variability, and more extraordinary occurrences is suspected to be caused by global warming [1]–[4]. Variability and extreme precipitation cause rain to become irregular [5], [6]. Concentrated rain results in extreme wet conditions, which triggered floods and landslides [7], [8]. However, prolonged dry spells can cause severe droughts [9]–[12]. These conditions significantly affect short- and long-term agricultural productivity[13]–[15]. Therefore, farmers are urged to understand climate change and its potential impacts to take adaptive measures to sustain farming businesses [16], [17].

The WMO and WCRP collaborated to create the Expert Team on Climate Change Detection and Indices (ETCCDI) by establishing 27 indices to evaluate extreme climate change globally in a particular area [18], [19]. The indices recommended by the ETCCDI have been widely used for random intense climate index research to detect global climate change in Asia [20]–[26], Africa [27]–[29], America [30] and Europe [31]–[34].

This research aims to assess extreme precipitation as a basis for planning adaptation strategies of the agricultural sector in the Selo watershed, Tanah Datar Regency, West Sumatra Province. Adaptation to water resources due to climate variability and change needs to be conducted because the Selo watershed is a center for agriculture to support the food needs of the community in Tanah Datar Regency, where the threat to food security due to crop failure is triggered by extreme precipitation events. Besides extreme precipitation factors, the selection of adaptation strategies also needs to consider the topographic conditions of the local location.

The Selo watershed has not experienced much land change due to migration. Hence, it is an excellent location to study the occurrence of extreme precipitation due to climate variability. The findings are expected to illustrate the impact of global climate change at the local scale, such as in the Selo watershed.

II. Material and Method

A. Research Location

This research was conducted in the Selo watershed, situated in the administrative region of Tanah Datar Regency and encompassing eight sub-districts, namely Salimpaung, Sungayang, Sungai Tarab, Pariangan, Lima Kaum, Rambatan, Padang Ganting, and Tanjung Emas. This watershed serves as a catchment and drainage area for water from the Selo River. Furthermore, the Selo River originates from Mount Marapi's southeastern slope and Mount Sago's southwestern slope, ultimately joining the Sinamar River around the Tanjung Emas Sub-district.

The Selo River typically follows a dendritic flow pattern with a southeast direction from its source, with more closely spaced tributaries in the western upstream area, as seen in Figure 1. The watershed receives an annual precipitation of 2000 mm based on climatological data. Meanwhile, the topographic assessment shows highly varied slopes, with most areas categorized as gentle to steep and very steep. Flat slopes are primarily located downstream, while paddy fields are concentrated in the central part of the Selo watershed. The soil in this area is mostly cambisol and podzolic, with gentle to moderately steep slopes.

B. Data

This research used reanalyzed precipitation information in grid format due to the limitations of in-situ observation data at the location [35]–[37]. The performance test was to evaluate extreme precipitation as performed in previous results [38]–[41]. This research used precipitation data from the CHIRPS model from 1981 to 2020 (http://chg.geog.ucsb.edu/data/chirps/index.html). The product was available in grid format, starting from 1981, with daily temporal and 0.05^{O} x 0.05^{O} spatial resolutions [42]. The validation results against observed data at precipitation stations showed that CHIRPS had the best performance compared to other products at monthly and annual time scales in tropical [43], [44], and sub-tropical [45]–[48] areas. Therefore, it could be recommended as research data for hydro climatology.

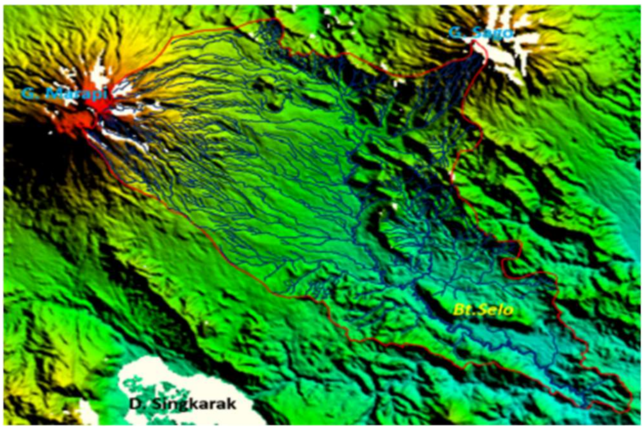

Fig. 1 Digital Elevation Model (DEM) for the Batang Selo watershed area source: SRTM imagery and Topographic Map of Indonesia.

C. Data Processing and Analysis

1) Downscaling Data: The processing stages started with CHIRPS data downscaling and extraction for the Selo watershed. Downscaling was done by remapping using bilinear interpolation in the climate data operator/CDO application [49] to create a grid of 0.025^{O} x 0.025^{O} [50].

2) Data Extraction: Data extraction was conducted at the grid points of the remapping data, as shown in Figure 2, and the result was time series data at a predetermined extraction point. The data extraction was performed using the Grid Analysis and Display System/GrADS software. The data were used as inputs in the RClimDex application to calculate the values and trends of extreme precipitation indices [51]–[53].

3) CHIRPS Data Validation: The accuracy assessment of CHIRPS data was conducted by comparing it with the sample data of in-situ precipitation observation points in the Selo watershed. The indicators used to evaluate the performance were the correlation coefficient (R), percent bias (PBias), RMSE-observation Standard deviation Ratio (RSR), and Nash-Sutcliffe Efficiency coefficient (NSE). Furthermore, the range of R, Pbias, RSR, and NSE was 0-1, $-\infty$ - ∞, 0 - ∞, and $-\infty$ - 1, with the best value being 1, 0, 0, and 1, respectively [35], [54], [55].

4) Extreme Precipitation Index: The extreme precipitation assessment was carried out using indices recommended by ETCCDI, such as PRCPTOT, CDD, CWD, SDII, R95p, R99p, RX1D, RX5D, R10mm, R20mm, R30mm, and R40mm. These indices were widely used to describe abnormal changes in precipitation conditions, including the total, duration, and frequency of extreme precipitation, as an indication of climate change [21], [28], [29], [37], [56], [57].

5) Trend Significance Analysis: In this research, a trend significance analysis and test were performed to determine the significance of changes in extreme precipitation. The trend significance in the extreme precipitation indices was calculated using the statistical method of the Mann-Kendall test, with the condition that the trend change was significant when the value of $|Z| \geq 1.96$ at a 95% confidence level. This test was widely used to detect trends in hydrological and climatological series [58]–[61].

6) Spatial Analysis: The final step of data processing was to perform a spatial analysis of the values, trends, and significance of the extreme precipitation indices. These spatial data were processed using Spatial Analysis in the ArcGIS software [62].

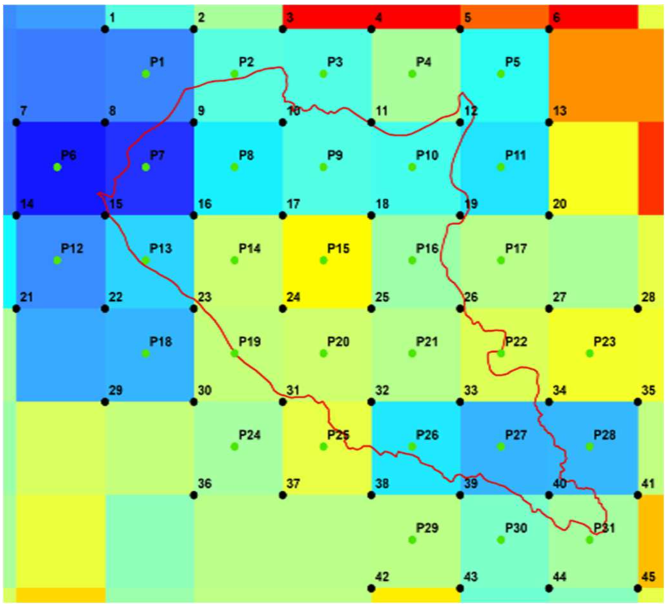

Fig. 2 The points in the middle of the grid (green dots) are the points (latitude-longitude) for data extraction.

III. Results and Discussion

A. Results

1) CHIRPS validation: The results of the CHIRPS accuracy performance assessment at several in-situ precipitation observation locations are shown in Table 1. The Salimpaung observation location is in the upstream area of the watershed; Sungai Tarab and Rambatan are in the middle area, while Saruaso and Padang Ganting are in the downstream area. Based on the indicators, the best performance is at the Salimpaung location. Meanwhile, the other sites show similar conditions with poor performance, as indicated by the high bias values between the CHIRPS and in-situ observation data. The CHIRPS model accurately views monthly and annual average precipitation data but cannot capture daily heavy events. This is evident from the trend of overestimating the precipitation frequency but underestimating its intensity compared to in situ observation data. Therefore, assessing the annual precipitation total (PRCPTOT) at the 95th percentile (R95p) is recommended. It is not recommended to determine daily heavy precipitation (R50mm, RX1D, RX5D) and total at the 99th percentile [57], [63], [64].

TABLE I
PERFORMANCE TEST INDICATORS FOR CHIRPS DATA

In situ observation	Data period	Corr	PBias	RSR	NSE
Salimpaung	2012-2020	0.44**	-1.41	0.96	0.07
Sungai Tarab	2009-2020	0.49**	42.20	1.20	-0.46
Rambatan	2013-2020	0.36**	39.34	1.23	-0.52
Saruaso	2014-2020	0.44**	37.92	1.28	-0.60
Padang Ganting	2012-2020	0.42**	35.34	1.13	-0.30

Source of in situ observation data: West Sumatra Climatology Station
** significant at a 99% significance level

2) Extreme precipitation assessment

- Prcptot index

The Selo watershed received average annual precipitation (precipitation total/Prcptot) between 1,800 and 2,600 mm from 1981 to 2020. Upstream, the precipitation ranged from 1,800 to 2,200 mm/year, while downstream, it was approximately 2,400 to 2,600 mm/year. Furthermore, the Prcptot index increased during the 1981-2020 period with a trend between 11.62 and 16.76 mm/year. The upstream part had the lowest increase trend, with a slope of 11.62 to 12.65 mm/year. However, the downstream part had the highest increase trend with a slope ranging from 15.73 to 16.76 mm/year. The trend significance test showed that the increasing annual precipitation trend was significant at a 95% confidence in the entire Selo watershed area. Fig. 3 shows the spatial analysis of the change significance in the Prcptot index.

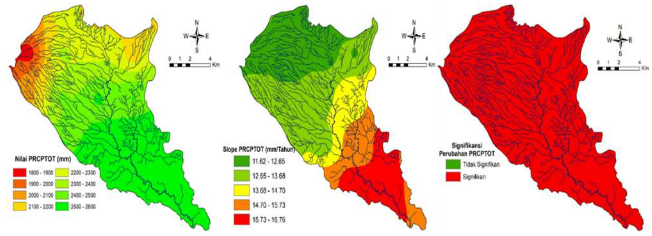

Fig. 3 Change significance in the amount of annual precipitation (prcptot) in the Selo watershed for the period 1981-2020.

- CDD index

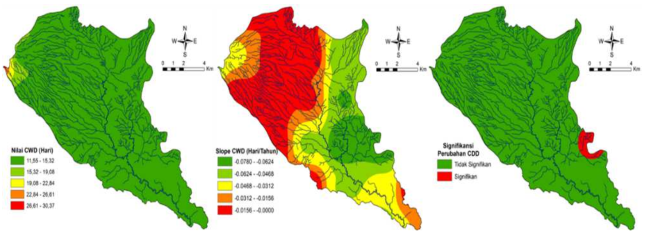

Fig. 4 Change significance in the vast number of CDD per year in the Selo watershed from 1981 to 2020.

The maximum Consecutive Dry Days (CDD) in the Selo watershed ranged from 11.55 to 15.32 days per year, with a small area upstream having longer CDD. Moreover, the CDD in the watershed had a negative trend, indicating a decrease in the number of CDDs, with the highest trend of 0.078 days/year. The results of the trend significance test showed that the change in CDD is generally insignificant. The spatial analysis of the significance of CDD index changes is shown in Fig. 4.

- CWD index

The average annual Consecutive Wet Days (CWD) ranged from 17.90 to 20.30 days per year, with the central part having lower CWD from 17.90 to 18.86 days per year and the upstream and downstream parts having more CWD. The CWD increased with a positive trend from 1981-2020, with a trend value ranging from 0.0911 to 0.2740 days per year. The significance test showed that the trend in changes in CWD was significant in most of the Selo watershed area. Fig. 5 shows the spatial distribution of values, trends, and significance of changes in CWD.

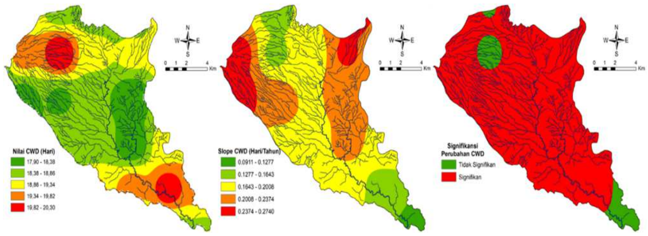

Fig. 5 Change significance in the longest CWD in the Selo watershed during the 1981-2020 period.

- SDII index

The Simple Daily Intensity Index (SDII) represents daily precipitation intensity. The SDII index values in the Selo watershed area ranged from 8.40 to 11.90 mm/day, with the lowest values distributed in the upstream area and the highest in the downstream. From 1981 to 2020, the SDII index increased with a trend ranging from 0.00 to 0.05 mm/day per year. Furthermore, Fig. 6 shows the spatial distribution of values, trends, and significance of changes in the SDII index, where significant changes are observed in most of the Selo watershed area.

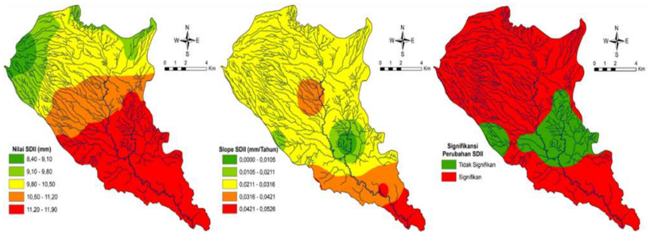

Fig. 6 Change significance in daily precipitation intensity per year (SDII) in the Selo watershed from 1981 to 2020.

- RX1D index

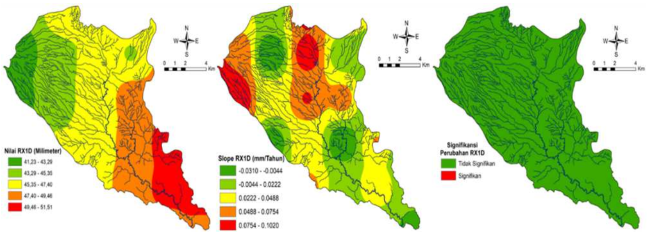

Fig. 7 Change significance in the maximum daily precipitation (RX1D) in the Selo watershed area for 1981-2020

The maximum daily precipitation amount (RX1D) ranged from 41.23 to 51.51 mm, with a spatial distribution pattern similar to the annual precipitation. The minimum value was observed in the upstream part of the watershed, while the maximum value was in the downstream position. The RX1D trend did not have a regular spatial distribution pattern, and some parts of the watershed had a negative trend, indicating a decrease in RX1D values. In contrast, others had a positive trend, indicating an increase. Fig. 7 displays the spatial distribution of the value, trend, and significance of the change in RX1D. However, significant changes in the RX1D trend were not observed in the entire Selo watershed area.

- RX5D index

The maximum precipitation amounts in 5 consecutive days (RX5D) ranged from 108.0 to 128.0 mm, with a spatial distribution pattern similar to RX1D. The minimum value was observed in the upstream part of the watershed, and the maximum value was observed in the downstream part. RX5D had an increasing trend, with a value ranging from 0.00 to 0.39 and an irregular spatial distribution pattern of trend values. However, the significance test of the RX5D trend showed insignificant changes throughout the Selo watershed area in Fig. 8.

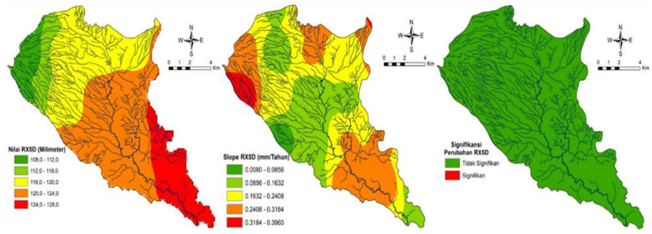

Fig. 8 Change significance in maximum precipitation in 5 consecutive days (RX5D) in the Selo watershed from 1981-2020.

- R95p index

The R95p index is the cumulative precipitation at the ≥95th percentile, indicating extremely wet conditions. In the Selo watershed, R95p values range from 301.8 to 390.5 mm, with a spatial distribution pattern similar to other precipitation amount indices, showing minimum and maximum values downstream of the watershed. The trend of R95p in the Selo watershed is positive, ranging from 0.84 to 6.48. However, the significance test of the R95p trend indicates that in most parts of the Selo watershed, the change in the R95p trend did not occur significantly. Fig. 9 shows the values, trend, and significance of the change in the R95p trend in the Selo watershed from 1981 to 2020.

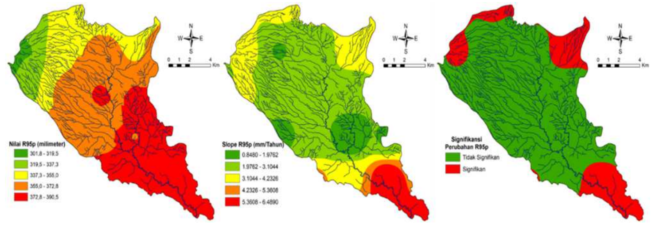

Fig. 9 Change significance in the annual 95th percentile of precipitation (R95p) in the Selo watershed from 1981-2020.

- R99p index

The R99p Index represents the cumulative precipitation at a percentile ≥99. The R99p values ranged from 82.71 - 106.33 mm, and the spatial distribution pattern of R99p was similar to that of other precipitation indices, with minimum values upstream and maximum values downstream of the watershed. The R99p index highlighted a positive trend, with values ranging from 0.004-1.43. However, the significance test of the R99p trend indicated that the change in most parts of the Selo watershed is insignificant. Fig. 10 shows the value, trend, and significance of the change in the R99p trend in the Selo watershed.

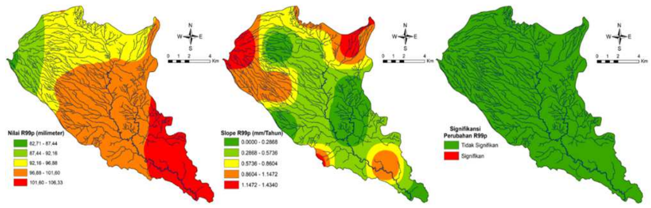

Fig. 10 Change significance in the annual precipitation percentile of 99 (R99p) in the Selo watershed from 1981 to 2020.

- R10mm index

The R10mm Index represents the number of days with precipitation amounts ≥10 mm/day in a year. 1981-2020, the R10mm index value ranged from 66.80 to 108.97 days/year. The spatial distribution of the minimum value occurred in the upstream area, while the maximum value occurred downstream. Over the data period, the R10mm index showed a positive trend with an R10mm trend value ranging from 0.60-1.00 days/year. The significance test indicated that the change in the R10mm trend in the entire Selo watershed was significant. Fig. 11 shows the spatial distribution of the significance of the change in the R10mm trend index.

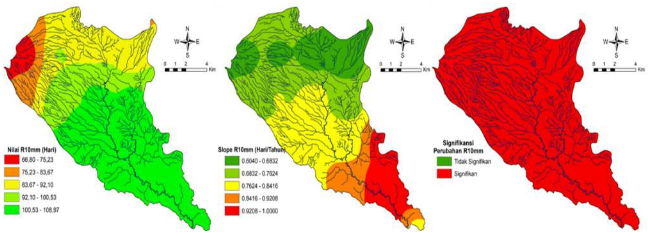

Fig. 11 Change significance in the number of days with precipitation of ≥10 mm/day (R10mm) in the Selo Watershed from 1981 to 2020

- R20mm index

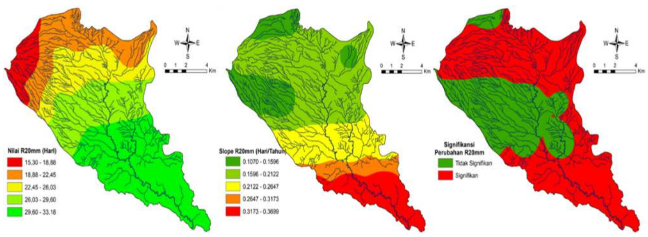

Fig. 12 Change significance in the number of days with precipitation of ≥20 mm/day (R20mm) in the Selo Watershed from 1981 to 2020

The R20mm Index represents the number of days with precipitation ≥20 mm/day per year. During the 1981-2020 period, the R20mm index value ranged from 15.30 to 33.18 days per year, with minimum and maximum values occurring upstream. Over the data period, the R20mm index showed a positive trend, with an R20mm trend value ranging from 0.10-0.36 days/year. Furthermore, the significance test indicated that the change in the R20mm trend in the entire Selo watershed is significant. Fig. 12 shows the spatial distribution of the significance of the change in the R20mm trend index.

- R30mm index

The R30mm Index represents the number of rainy days with precipitation ≥30 mm/day in a year. From 1981-2 to 20, the R30mm index ranged from 3.44 to 8.59 days per year, with minimum and maximum values occurring upstream. Over the data period, the R30mm index exhibited a positive trend, ranging from 0.00 to 0.11 days/year. Furthermore, the significance test indicated that the change in trend for R30mm only occurred significantly in a small downstream area of the Selo watershed. Fig.13 shows the spatial distribution of the significance of the change in trend for the R30mm index.

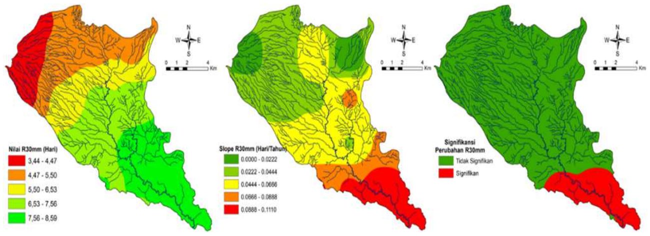

Fig. 13 Change significance in the number of days with precipitation of ≥30 mm/day (R30mm) in the Selo watershed from 1981 to 2020.

- R40mm index

The R40mm index represents the number of days with a precipitation amount of ≥40 mm/day in a year. The range of R40mm index values in the Selo watershed from 1981-2020 was from 0.80 to 2.30 days per year, with the minimum value occurring upstream and the maximum occurring downstream. There was no significant change in the R40mm index value during the research period. The spatial distribution of the R40mm index values, trends, and significance are shown in Fig. 14.

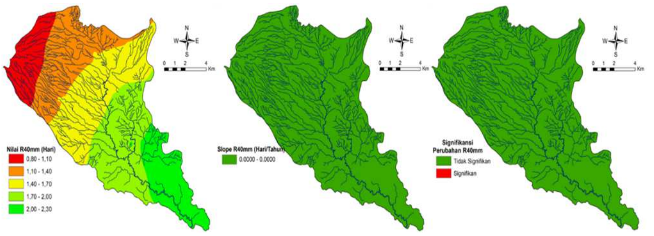

Fig. 14 Change significance in the number of days with precipitation of ≥40 mm/day (R40mm) in the Selo watershed from 1981 to 2020

B. Discussion

1) Trend of extreme precipitation indices in the Selo watershed: Based on the results, overall extreme precipitation indices in the Selo watershed indicate a trend towards wet conditions during the period 1981-2020, as shown in Table 2. Indices indicating a trend towards wet conditions also have a positive tendency. CWD and CDD as an index to describe wet and dry conditions have a positive and negative trend. Based on the significance test, there is a trend for indices that indicate wet conditions such as PRCPTOT, CWD, SDII, R10mm, and R20mm. However, the changes in wet conditions do not occur in very wet and extremely wet conditions, as indicated by the lack of significant changes in R95p, R99p, R30mm, and R40mm.

TABLE II
TREND SIGNIFICANCE OF EXTREME PRECIPITATION INDICES IN THE SELO WATERSHED

Extreme Precipitation Indices	Trend	Significance
PRCPTOT	+	Significant in all areas of the watershed
CDD	-	Significant in a small area of the watershed
CWD	+	Significant in most areas of the watershed
SDII	+	Significant in most areas of the watershed
RX1D	+	Insignificant
RX5D	+	Insignificant
R95p	+	Significant in a small area of the watershed

Extreme Precipitation Indices	Trend	Significance
R99p	+	Insignificant
R10mm	+	Significant in all areas of the watershed
R20mm	+	Significant in most areas of the watershed
R30mm	+	Significant in a small area of the watershed
R40mm	+	Insignificant

As a comparison to the results of the extreme precipitation indices assessment in the Selo Watershed, Table 3 shows some assessment results with similar data and methods. The summary of the results indicates a positive trend in the indices, showing an increase in wet conditions. Overall, this research recommends using CHIRPS data to assess extreme precipitation conditions based on the cumulative amount of precipitation. CHIRPS is not responsive to heavy precipitation events within 24 hours.

TABLE III
RESULTS OF EXTREME PRECIPITATION INDEX RESEARCH IN OTHER AREAS

Areas	Author	Summary of previous research findings
Amazon, Brazil	[57]	The research utilized CHIRPS and in situ observation precipitation data in Brazil's Amazon region. Based on the research outcomes, CHIRPS data was recommended to be used to evaluate annual precipitation trends in the region. However, the research concluded that the data was not used for assessing daily precipitation trends.
West Africa	[64]	The research employs CHIRPS data in several West African countries, including Senegal, Niger, Burkina Faso, Ivory Coast, and Benin. The findings indicated a positive trend (+) in all extreme precipitation indices, except for CDD, which exhibited a negative trend (-). The research recommended using CHIRPS data to assess annual precipitation trends in the region instead of daily trends.
Jalisco (Mexico)	[63]	The research employed CHIRPS data to evaluate precipitation trends in Jalisco, Mexico. The results indicated an increasing trend in RX1D, RX5D, CWD, R95p, and SDII indices. However, based on other findings, CHIRPS data was unsuitable for detecting heavy precipitation events within 24 hours (daily).
Amazon	[65]	The research employed CHIRPS data to examine precipitation trends in the Amazon region. The findings indicated an increasing trend in annual extreme precipitation indicators in the wet and dry seasons. However, the research showed that several precipitation frequency indicators, such as CWD and CDD, were season-dependent, with CDD exhibiting a negative trend (-) during the dry season.

The persistent atmospheric dynamic conditions greatly influence precipitation in a particular area. This persistence is strongly affected by the scale of atmospheric dynamics and the local conditions of the respective area, including critical changes such as changes in extensive land cover. These conditions greatly affect the characteristics and the typology of extreme precipitation in an area [65], [66].

The location in a shadow area causes the watershed to receive relatively less precipitation than West Sumatra's western coastal area. Climatologically, rainfall in the Selo watershed has an inland type opposite to the coastal style. Inland type is not strongly correlated with changes in wind speed in the lower tropospheric layer [67]. The precipitation data and global climate indices show that the conditions in the Selo watershed are more strongly affected by anomalies in sea surface temperatures (SST) in the Pacific and Indian Oceans, such as the Oceanic Nino Index (ONI), Nino3.4, and Dipole Mode Index (DMI), compared to monsoon winds. These include Australian Monsoon Index (AUSMI), the South Asian Monsoon Index (SAMI), Western North Pacific Monsoon Index (WNPMI), and Indian Monsoon Index (IMI).

2) The trend of wet/dry conditions in the Selo watershed: The annual precipitation total in the Selo watershed during the period 1981-2020 indicates that in the first two decades (1981-1990 and 1991-2000), there was a decrease in precipitation total by 6.3% in 1981-1990 and 9.4% in 1991-2000. In the last two decades (2001-2010 and 2011-2020), precipitation in the watershed increased by about 9.6% in 2001-2010 and about 6.2% in 2011-2020. Therefore, 1981-1990 and 1991-2000 are dry decades, while 2001-2010 and 2011-2020 are wet. The trend of wet conditions in the Selo watershed is also evident from [68] regarding the variability of wet and dry conditions using the Meteorological Drought Index (SPI and SPEI) assessment method. The results show a trend of wet conditions, specifically in the last two decades of 1981-2020, as shown in Figure 15. Furthermore, dry conditions occur more frequently than wet conditions during 1981-1990 and 1991-2000. The opposite has occurred in the last two decades, where wet conditions occur more frequently. Moreover, the percentage of dry, wet, and normal conditions is highest during 1991-2000, 2001-2010, and 1981-1990, respectively.

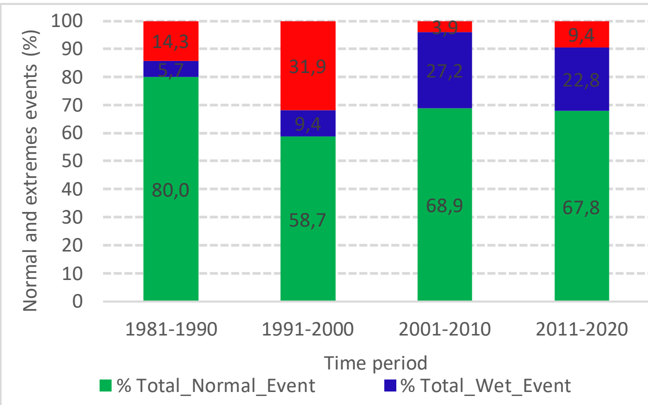

Fig 15 The percentage of normal conditions and extreme events (wet/dry) per decade in the Selo watershed from 1981 to 2020.

3) Extreme precipitation assessment results and proposed adaptation strategies: The extreme precipitation assessment shows a trend of wet conditions indices, particularly in the past two decades. The significance test indicates the extreme precipitation indices based on the total experience increase. Therefore, there is a trend for the annual precipitation total to remain constant or slightly increase. Still, its variability is high, indicating that the frequency is irregular or uneven at certain times. The observed conditions can be a fundamental basis for determining an area's most suitable adaptation strategy.

The trend of wet conditions, soil type, land slope with an uneven trend, and land cover conditions require certain agricultural land cultivation treatments. The trend towards wetter conditions on agricultural land with uneven slopes increases the risk of surface runoff, soil nutrient loss, and soil fertility damage due to topsoil layer erosion. Therefore, implementing adaptation strategies to prevent these issues is crucial. One potential approach is the implementation of techno-ecological agriculture based on soil and water conservation to minimise or even prevent the loss of water and soil nutrients.

According to the data processing results for 2010-2020, there has been a significant shift in land use in the Selo watershed. The area dedicated to rice fields has increased by 6.75%, while housing has expanded by 2.44%, accounting for a total of 16.93% of land use area that has undergone changes or conversion (https://dbgis.menlhk.go.id/portal/home/webmap/viewer.htm, accessed on March 5, 2023). The important point of this land use conversion is the change in cover types and the increase in the consumption of water resources for agricultural and household purposes. The main factor causing land degradation is the change of vegetative to non-vegetative cover types, such as housing. These cover types increase water runoff and reduce infiltration into soil pores to become groundwater. Increasing rice field areas is necessary to fulfill food needs and improve food security. The conversion of land to rice fields and housing may have consequences for the availability of water resources for agricultural purposes. The increase in housing also indicates a rise in the number of households, resulting in a corresponding increase in domestic water consumption.

Effective water resource management demands an integrated and comprehensive approach that considers the needs of different areas within the watershed. This approach should incorporate various measures for sustainable water use, conservation, and preservation. To this end, water management policies in the upstream area should maintain soil hydrological functions by implementing conservation methods to preserve the hydrological function. However, the policies in the middle and downstream areas prioritise promoting efficient water use through conservation methods. It is essential to acknowledge the significance of equitable distribution of water resources while promoting conservation and sustainability. By considering water requirements for agriculture and domestic purposes, integrated policies are implemented from the upstream area as a water catchment and infiltration zone to the middle and downstream areas as a conservation-based adaptation alternative [69]. Some recommended adaptation strategies include land conservation to maintain and restore hydrological functions in the upstream area of the watershed as well as water-saving through rainwater harvesting and storage. To control land degradation with soil nutrient loss, mechanical and vegetative soil erosion control must be conducted [70], [71].

IV. Conclusion

The results of data processing, analysis, and discussion regarding extreme precipitation assessment in the Selo watershed lead to the following conclusions: the CHIRPS data are recommended for assessing extreme precipitation based on monthly and annual total or average, such as PRCPTOT. However, it is not recommended for assessing extreme precipitation based on daily intensity, such as RX1D and RX5D. The assessment of extreme precipitation indices indicates a trend toward wet conditions in the area. This is indicated by the indices for the wet conditions category, such as the increasing trend of annual PRCPTOT, increasing number of CWD, and decreasing number of CDD.

The assessment also indicates that the annual precipitation total tends to increase irregularly. The wet conditions with increasing annual precipitation total and varying frequency, combined with the topography of the watershed, can serve as the basis for selecting adaptation strategies for the agricultural water resources sector. One option is a conservation-based adaptation that integrates with comprehensive watershed management. The findings indicating a trend of increasing wet conditions are expected to become the basis for policy directions in determining adaptation strategies of water resources for agriculture in the Selo watershed to stakeholders.

Acknowledgment

The authors appreciate the Climate Hazards Center, University of California, Santa Barbara, USAID, and the Department of Geography, University of California, Santa Barbara, for providing the CHIRPS precipitation model data.

References

[1] M. H. I. Dore, “Climate change and changes in global precipitation patterns: What do we know?,” Environment International, vol. 31, no. 8, pp. 1167–1181, Oct. 2005, doi: 10.1016/j.envint.2005.03.004.

[2] A. K. Mishra, “Quantifying the impact of global warming on precipitation patterns in India,” Meteorological Applications, vol. 26, no. 1, pp. 153–160, Nov. 2018, doi: 10.1002/met.1749.

[3] Z. Li, X. Li, Y. Wang, and S. M. Quiring, “Impact of climate change on precipitation patterns in Houston, Texas, USA,” Anthropocene, vol. 25, p. 100193, Mar. 2019, doi: 10.1016/j.ancene.2019.100193.

[4] A. Rahmat, M. Khoiru Zaki, I. Effendi, A. Mutolib, H. Yanfika, and I. Listiana, “Effect of global climate change on air temperature and precipitation in six cities in Gifu Prefecture, Japan,” Journal of Physics: Conference Series, vol. 1155, p. 012070, Feb. 2019, doi: 10.1088/1742-6596/1155/1/012070.

[5] M. J. Khordadi, A. Alizadeh, M. Nassiri Mahallati, H. Ansari, and H. Sanaeinejad, “Climate Change Impact on Precipitation Extreme Events in Uncertainty Situation; Passing from Global Scale to Regional Scale,” International Journal of Engineering, vol. 28, no. 8, Aug. 2015, doi: 10.5829/idosi.ije.2015.28.08b.05.

[6] B. Clarke, F. Otto, R. Stuart-Smith, and L. Harrington, “Extreme weather impacts of climate change: an attribution perspective,” Environmental Research: Climate, vol. 1, no. 1, p. 012001, Jun. 2022, doi: 10.1088/2752-5295/ac6e7d.

[7] H. Tabari, “Climate change impact on flood and extreme precipitation increases with water availability,” Scientific Reports, vol. 10, no. 1, Aug. 2020, doi: 10.1038/s41598-020-70816-2.

[8] J. R. Araújo, A. M. Ramos, P. M. M. Soares, R. Melo, S. C. Oliveira, and R. M. Trigo, “Impact of extreme rainfall events on landslide activity in Portugal under climate change scenarios,” Landslides, vol. 19, no. 10, pp. 2279–2293, Jun. 2022, doi: 10.1007/s10346-022-01895-7.

[9] K. E. Trenberth et al., “Global warming and changes in drought,” Nature Climate Change, vol. 4, no. 1, pp. 17–22, Dec. 2013, doi: 10.1038/nclimate2067.

[10] J. Carrillo, S. Hernández-Barrera, F. J. Expósito, J. P. Díaz, A. González, and J. C. Pérez, “The uneven impact of climate change on drought with elevation in the Canary Islands,” npj Climate and Atmospheric Science, vol. 6, no. 1, Apr. 2023, doi: 10.1038/s41612-023-00358-7.

[11] X. Yuan, Y. Wang, P. Ji, P. Wu, J. Sheffield, and J. A. Otkin, “A global transition to flash droughts under climate change,” Science, vol. 380, no. 6641, pp. 187–191, Apr. 2023, doi: 10.1126/science.abn6301.

[12] J. P. C. Eekhout, J. E. Hunink, W. Terink, and J. de Vente, “Why increased extreme precipitation under climate change negatively affects water security,” Hydrology and Earth System Sciences, vol. 22, no. 11, pp. 5935–5946, Nov. 2018, doi: 10.5194/hess-22-5935-2018.

[13] A. A. Chandio, Y. Jiang, A. Rehman, and A. Rauf, “Short and long-run impacts of climate change on agriculture: an empirical evidence from China,” International Journal of Climate Change Strategies and Management, vol. 12, no. 2, pp. 201–221, Jan. 2020, doi: 10.1108/ijccsm-05-2019-0026.

[14] Z. Shi, H. Huang, Y. Wu, Y.-H. Chiu, and S. Qin, “Climate Change Impacts on Agricultural Production and Crop Disaster Area in China,” International Journal of Environmental Research and Public Health, vol. 17, no. 13, p. 4792, Jul. 2020, doi: 10.3390/ijerph17134792.

[15] M. S. Kukal and S. Irmak, “Climate-Driven Crop Yield and Yield Variability and Climate Change Impacts on the U.S. Great Plains Agricultural Production,” Scientific Reports, vol. 8, no. 1, Feb. 2018, doi: 10.1038/s41598-018-21848-2.

[16] A. A. Mamun et al., “Smallholder Farmers’ Perceived Climate-Related Risk, Impact, and Their Choices of Sustainable Adaptation Strategies,” Sustainability, vol. 13, no. 21, p. 11922, Oct. 2021, doi: 10.3390/su132111922.

[17] D. Etana, D. J. R. M. Snelder, C. F. A. van Wesenbeeck, and T. de Cock Buning, “The Impact of Adaptation to Climate Change and Variability on the Livelihood of Smallholder Farmers in Central Ethiopia,” Sustainability, vol. 13, no. 12, p. 6790, Jun. 2021, doi: 10.3390/su13126790.

[18] L. V. Alexander et al., “Global observed changes in daily climate extremes of temperature and precipitation,” Journal of Geophysical Research: Atmospheres, vol. 111, no. D5, Mar. 2006, doi: 10.1029/2005jd006290.

[19] M. G. Donat et al., “Changes in extreme temperature and precipitation in the Arab region: long-term trends and variability related to ENSO and NAO,” International Journal of Climatology, vol. 34, no. 3, pp. 581–592, May 2013, doi: 10.1002/joc.3707.

[20] D. Vinod and A. Mahesha, “Spatiotemporal Analysis of Precipitation-based ETCCDI Indicators over India,” Apr. 2023, doi: 10.21203/rs.3.rs-2779617/v1.

[21] A. S. Bhatti et al., “Trend in Extreme Precipitation Indices Based on Long Term In Situ Precipitation Records over Pakistan,” Water, vol. 12, no. 3, p. 797, Mar. 2020, doi: 10.3390/w12030797.

[22] X. Wang, Y. Li, M. Yan, and X. Gong, “Changes in temperature and precipitation extremes in the arid regions of China during 1960–2016,” Frontiers in Ecology and Evolution, vol. 10, Jul. 2022, doi: 10.3389/fevo.2022.902813.

[23] Supari, F. Tangang, L. Juneng, and E. Aldrian, “Observed changes in extreme temperature and precipitation over Indonesia,” International Journal of Climatology, vol. 37, no. 4, pp. 1979–1997, Jul. 2016, doi: 10.1002/joc.4829.

[24] A. Limsakul and P. Singhruck, “Long-term trends and variability of total and extreme precipitation in Thailand,” Atmospheric Research, vol. 169, pp. 301–317, Mar. 2016, doi: 10.1016/j.atmosres.2015.10.015.

[25] D. Zhang, W. Wang, S. Liang, and S. Wang, “Spatiotemporal Variations of Extreme Precipitation Events in the Jinsha River Basin, Southwestern China,” Advances in Meteorology, vol. 2020, pp. 1–13, Oct. 2020, doi: 10.1155/2020/3268923.

[26] M. L. Felix et al., “Detailed Trend Analysis of Extreme Climate Indices in the Upper Geum River Basin,” Water, vol. 13, no. 22, p. 3171, Nov. 2021, doi: 10.3390/w13223171.

[27] M. O. Audu, F. N. Okeke, and T. Igbawua, “Analyses of Spatial Distribution and Temporal Trends of Temperature and Its Extremes over Nigeria using Climate Indices,” Trends in Sciences, vol. 19, no. 13, p. 4635, Jun. 2022, doi: 10.48048/tis.2022.4635.

[28] M. Fofana et al., “Urban flash flood and extreme rainfall events trend analysis in Bamako, Mali,” Environmental Challenges, vol. 6, p. 100449, Jan. 2022, doi: 10.1016/j.envc.2022.100449.

[29] D. A. Vondou, G. M. Guenang, T. L. A. Djiotang, and P. H. Kamsu-Tamo, “Trends and Interannual Variability of Extreme Rainfall Indices over Cameroon,” Sustainability, vol. 13, no. 12, p. 6803, Jun. 2021, doi: 10.3390/su13126803.

[30] A. K. Cooley and H. Chang, “Detecting change in precipitation indices using observed (1977–2016) and modeled future climate data in Portland, Oregon, USA,” Journal of Water and Climate Change, vol. 12, no. 4, pp. 1135–1153, Jun. 2020, doi: 10.2166/wcc.2020.043.

[31] M. Abdellatif, W. Atherton, and R. Alkhaddar, “Climate Change Impacts on the Extreme Rainfall for Selected Sites in North Western England,” Open Journal of Modern Hydrology, vol. 02, no. 03, pp. 49–58, 2012, doi: 10.4236/ojmh.2012.23007.

[32] C. Ryan, M. Curley, S. Walsh, and C. Murphy, “Long-term trends in extreme precipitation indices in Ireland,” International Journal of Climatology, vol. 42, no. 7, pp. 4040–4061, Dec. 2021, doi: 10.1002/joc.7475.

[33] F. Domínguez-Castro et al., “A multidecadal assessment of climate indices over Europe,” Scientific Data, vol. 7, no. 1, Apr. 2020, doi: 10.1038/s41597-020-0464-0.

[34] T. Popov, S. Gnjato, G. Trbić, and M. Ivanišević, “Trends in extreme daily precipitation indices in Bosnia and Herzegovina,” Zbornik radova - Geografski fakultet Univerziteta u Beogradu, no. 65–1a, pp. 5–24, 2017, doi: 10.5937/zrgfub1765005p.

[35] I. Bamweyana, M. Musinguzi, and L. M. Kayondo, “Evaluation of CHIRPS Satellite Gridded Dataset as an Alternative Rainfall Estimate for Localized Modelling over Uganda,” Atmospheric and Climate Sciences, vol. 11, no. 04, pp. 797–811, 2021, doi: 10.4236/acs.2021.114046.

[36] E. M. C. Demaria et al., “Using a Gridded Global Dataset to Characterize Regional Hydroclimate in Central Chile,” Journal of Hydrometeorology, vol. 14, no. 1, pp. 251–265, Feb. 2013, doi: 10.1175/jhm-d-12-047.1.

[37] Y.-S. Tung, C.-Y. Wang, S.-P. Weng, and C.-D. Yang, “Extreme index trends of daily gridded rainfall dataset (1960–2017) in Taiwan,” Terrestrial, Atmospheric and Oceanic Sciences, vol. 33, no. 1, Mar. 2022, doi: 10.1007/s44195-022-00009-z.

[38] B. Timmermans, M. Wehner, D. Cooley, T. O’Brien, and H. Krishnan, “An evaluation of the consistency of extremes in gridded precipitation data sets,” Climate Dynamics, vol. 52, no. 11, pp. 6651–6670, Jan. 2019, doi: 10.1007/s00382-018-4537-0.

[39] Q. He et al., “Evaluation of Extreme Precipitation Based on Three Long-Term Gridded Products over the Qinghai-Tibet Plateau,” Remote Sensing, vol. 13, no. 15, p. 3010, Jul. 2021, doi: 10.3390/rs13153010.

[40] A. D. King, L. V. Alexander, and M. G. Donat, “The efficacy of using gridded data to examine extreme rainfall characteristics: a case study for Australia,” International Journal of Climatology, vol. 33, no. 10, pp. 2376–2387, Sep. 2012, doi: 10.1002/joc.3588.

[41] G. Hu and C. L. E. Franzke, “Evaluation of Daily Precipitation Extremes in Reanalysis and Gridded Observation-Based Data Sets Over Germany,” Geophysical Research Letters, vol. 47, no. 18, Sep. 2020, doi: 10.1029/2020gl089624.

[42] C. Funk et al., “The climate hazards infrared precipitation with stations—a new environmental record for monitoring extremes,” Scientific Data, vol. 2, no. 1, Dec. 2015, doi: 10.1038/sdata.2015.66.

[43] A. Pratama, H. M. Agiel, and A. A. Oktaviana, “Evaluasi Satellite Precipitation Product (GSMaP, CHIRPS, dan IMERG) di Kabupaten Lampung Selatan,” Journal of Science and Applicative Technology, vol. 6, no. 1, p. 32, Apr. 2022.

[44] N. F. Saragih et al., “Validation of CHIRPS Estimation Rainfall Data Using Numerical Accuracy Test with Precitipation Observation Data,” IOP Conference Series: Earth and Environmental Science, vol. 1083, no. 1, p. 012095, Sep. 2022, doi: 10.1088/1755-1315/1083/1/012095.

[45] J. Hsu, W.-R. Huang, P.-Y. Liu, and X. Li, “Validation of CHIRPS Precipitation Estimates over Taiwan at Multiple Timescales,” Remote Sensing, vol. 13, no. 2, p. 254, Jan. 2021, doi: 10.3390/rs13020254.

[46] V. Popovych and I. Dunaieva, “Assessment of the GPM IMERG and CHIRPS precipitation estimations for the steppe part of the Crimea,” Meteorology Hydrology and Water Management, Mar. 2021, doi: 10.26491/mhwm/133088.

[47] C. Ocampo-Marulanda, C. Fernández-Álvarez, W. L. Cerón, T. Canchala, Y. Carvajal-Escobar, and W. Alfonso-Morales, “A spatiotemporal assessment of the high-resolution CHIRPS rainfall dataset in southwestern Colombia using combined principal component analysis,” Ain Shams Engineering Journal, vol. 13, no. 5, p. 101739, Sep. 2022, doi: 10.1016/j.asej.2022.101739.\

[48] C. López-Bermeo, R. D. Montoya, F. J. Caro-Lopera, and J. A. Díaz-García, "Validation of the accuracy of the CHIRPS precipitation dataset at representing climate variability in a tropical mountainous region of South America," Physics and Chemistry of the Earth, Parts A/B/C, vol. 127, p. 103184, Oct. 2022, doi: 10.1016/j.pce.2022.103184.
[49] U. Schulzweida, L. Kornblueh, and R. Quast, "CDO User's Guide, Climate Data Operators Version 1.4.1," 2009.
[50] C. R. Rajulapati, S. M. Papalexiou, M. P. Clark, and J. W. Pomeroy, "The Perils of Regridding: Examples using a Global Precipitation Dataset," Journal of Applied Meteorology and Climatology, Oct. 2021, doi: 10.1175/jamc-d-20-0259.1.
[51] B. Xuebin Zhang et al., "RClimDex (1.0) User Manual," 2004.
[52] L. Alexander et al., "RClimDex (0.9) User Manual," 2004.
[53] Baljeet Kaur, Navneet Kaur, Sanjeev Kumar Kataria, and Sompal Singh, "Assessing the variability in temperature and rainfall extremes using RClimdex in Jalandhar district of Punjab," Journal of Agrometeorology, vol. 24, no. 4, pp. 437–439, Dec. 2022, doi: 10.54386/jam.v24i4.1749.
[54] D. N. Moriasi, J. G. Arnold, M. W. Van Liew, R. L. Bingner, R. D. Harmel, and T. L. Veith, "Model Evaluation Guidelines for Systematic Quantification of Accuracy in Watershed Simulations," Transactions of the ASABE, vol. 50, no. 3, pp. 885–900, 2007, doi: 10.13031/2013.23153.
[55] C. D. Geleta and T. A. Deressa, "Evaluation of Climate Hazards Group InfraRed Precipitation Station (CHIRPS) <scp>satellite-based</scp> rainfall estimates over Finchaa and Neshe Watersheds, Ethiopia," Engineering Reports, vol. 3, no. 6, Nov. 2020, doi: 10.1002/eng2.12338.
[56] E. Obada, E. A. Alamou, E. I. Biao, and E. B. J. Zandagba, "Interannual Variability and Trends of Extreme Rainfall Indices over Benin," Climate, vol. 9, no. 11, p. 160, Oct. 2021, doi: 10.3390/cli9110160.
[57] R. B. L. Cavalcante, D. B. da S. Ferreira, P. R. M. Pontes, R. G. Tedeschi, C. P. W. da Costa, and E. B. de Souza, "Evaluation of extreme rainfall indices from CHIRPS precipitation estimates over the Brazilian Amazonia," Atmospheric Research, vol. 238, p. 104879, Jul. 2020, doi: 10.1016/j.atmosres.2020.104879.
[58] A. Sanogo, R. S. Kabange, P. A. Owusu, B. I. Djire, R. F. Donkoh, and N. Dia, "Investigation into Recent Temperature and Rainfall Trends in Mali Using Mann-Kendall Trend Test: Case Study of Bamako," Journal of Geoscience and Environment Protection, vol. 11, no. 03, pp. 155–172, 2023, doi: 10.4236/gep.2023.113011.
[59] S. P Z and J. K V, "Comparative study of innovative trend analysis technique with Mann-Kendall tests for extreme rainfall," Arabian Journal of Geosciences, vol. 14, no. 7, Mar. 2021, doi: 10.1007/s12517-021-06906-w.
[60] A. Gadedjisso-Tossou, K. I. Adjegan, and A. K. M. Kablan, "Rainfall and Temperature Trend Analysis by Mann–Kendall Test and Significance for Rainfed Cereal Yields in Northern Togo," Sci, vol. 2, no. 4, p. 74, Sep. 2020, doi: 10.3390/sci2040074.
[61] S. Agarwal, A. S. Suchithra, and S. Pal Singh, "Analysis and Interpretation of Rainfall Trend using Mann-Kendall's and Sen's Slope Method," Indian Journal of Ecology, vol. Vol. 48 (2), pp. 453–457, 2021.
[62] ESRI, Using ArcGIS Spatial Analyst. Computer Software, 2001. [Online]. Available: www.esri.com.
[63] E. V. Garcia, J. C. M. Hernandez, M. de Lourdes Romo Aguilar, F. O. G. Concepción, and R. C. Aja, "Potential of the CHIRPS Database for Extreme Precipitation Risk Studies. Assessment in the State of Jalisco (Mexico)," International Journal of Sustainable Development and Planning, vol. 18, no. 3, pp. 847–855, Mar. 2023, doi: 10.18280/ijsdp.180320.
[64] D. Sacré Regis M. et al., "Using the CHIRPS Dataset to Investigate Historical Changes in Precipitation Extremes in West Africa," Climate, vol. 8, no. 7, p. 84, Jun. 2020, doi: 10.3390/cli8070084.
[65] B. M. Funatsu et al., "Assessing precipitation extremes (1981–2018) and deep convective activity (2002–2018) in the Amazon region with CHIRPS and AMSU data," Climate Dynamics, vol. 57, no. 3–4, pp. 827–849, Apr. 2021, doi: 10.1007/s00382-021-05742-8.
[66] N. Haghtalab, N. Moore, B. P. Heerspink, and D. W. Hyndman, "Evaluating spatial patterns in precipitation trends across the Amazon basin driven by land cover and global scale forcings," Theoretical and Applied Climatology, vol. 140, no. 1–2, pp. 411–427, Jan. 2020, doi: 10.1007/s00704-019-03085-3.
[67] J.-I. Hamada, M. D. Yamanaka, S. Mori, Y. I. Tauhid, and T. Sribimawati, "Differences of Rainfall Characteristics between Coastal and Interior Areas of Central Western Sumatera, Indonesia," Journal of the Meteorological Society of Japan. Ser. II, vol. 86, no. 5, pp. 593–611, 2008, doi: 10.2151/jmsj.86.593.
[68] S. Nugroho, R. Febriamansyah, E. G. Ekaputra, and D. Gunawan, "Investigation of the Variability of Dry / Wet Meteorological conditions using the SPEI / SPI Index in the Selo Watershed, Period 1981-2020," IOP Publishing, 2023.
[69] S. Arsyad, Konservasi Tanah & Air, Edisi Kedua. IPB Press, 2000.
[70] E. Obada, E. A. Alamou, E. I. Biao, and E. B. J. Zandagba, "Interannual variability and trends of extreme rainfall indices over benin," Climate, vol. 9, no. 11, Nov. 2021, doi: 10.3390/cli9110160.
[71] F. R. Troeh, J. A. (James A. Hobbs, and R. L. (Roy L. Donahue, Soil and water conservation : for productivity and environmental protection. Pearson/Education, 2004.